PTEP

Prog. Theor. Exp. Phys. **2016**, 00000 (19 pages)
DOI: 10.1093/ptep/0000000000

Impacts of B-factory measurements on determination of fragmentation functions from electron-positron annihilation data

M. Hirai[1,2], H. Kawamura[3,4], S. Kumano[4,5], and K. Saito[2]

[1]*Nippon Institute of Technology, Saitama 345-8501, Japan*
[2]*Department of Physics, Faculty of Science and Technology, Tokyo University of Science, 2641, Yamazaki, Noda, Chiba, 278-8510, Japan*
[3]*Department of Mathematics, Juntendo University, Inzai, Chiba 270-1695, Japan*
[4]*KEK Theory Center, Institute of Particle and Nuclear Studies, High Energy Accelerator Research Organization (KEK), 1-1, Ooho, Tsukuba, Ibaraki, 305-0801, Japan*
[5]*J-PARC Branch, KEK Theory Center, Institute of Particle and Nuclear Studies, KEK and Theory Group, Particle and Nuclear Physics Division, J-PARC Center, 203-1, Shirakata, Tokai, Ibaraki, 319-1106, Japan*

arXiv:1608.04067v2 [hep-ph] 27 Sep 2016

Fragmentation functions are determined for the pion and kaon by global analyses of charged-hadron production data in electron-positron annihilation. Accurate measurements were reported by the Belle and BaBar collaborations for the fragmentation functions at the center-of-mass energies of 10.52 GeV and 10.54 GeV, respectively, at the KEK and SLAC B factories, whereas other available e^+e^- measurements were mostly done at higher energies, mainly at the Z mass of 91.2 GeV. There is a possibility that gluon fragmentation functions, as well as quark fragmentation functions, are accurately determined by scaling violation. We report our global analysis of the fragmentation functions especially to show impacts of the B-factory measurements on the fragmentation function determination. Our results indicate that the fragmentation functions are determined more accurately not only by the scaling violation but also by high-statistical nature of the Belle and BaBar data. However, there are some tensions between the Belle and BaBar data in comparison with previous measurements. We also explain how the flavor dependence of quark fragmentation functions and the gluon function are separated by using measurements at different Q^2 values. In particular, the electric and weak charges are different depending on the quark type, so that a light-quark flavor separation also became possible in principle due to the precise data at both $\sqrt{s} \simeq 10.5$ GeV and 91.2 GeV.

Subject Index B65, C22, D32

1. Introduction

Semi-inclusive hadron production processes become increasingly important for probing hadrons and quark-gluon system properties and for finding a signature beyond the standard model in high-energy hadron reactions. For describing their cross sections, there are three ingredients: parton distribution functions (PDFs) of initial hadrons, intermediate partonic interactions, and fragmentation functions in the final state. The PDFs have been well investigated in a wide kinematical region with a variety of experimental measurements, and the partonic interactions can be calculated in perturbative QCD (Quantum Chromodynamics). However, the fragmentation functions have not been accurately determined as

© The Author(s) 2012. Published by Oxford University Press on behalf of the Physical Society of Japan.
This is an Open Access article distributed under the terms of the Creative Commons Attribution License (http://creativecommons.org/licenses/by-nc/3.0), which permits unrestricted use, distribution, and reproduction in any medium, provided the original work is properly cited.

it was typically shown in Ref. [1]. Namely, there are large uncertainty bands especially in disfavored-quark and gluon functions even in the pion, for which relatively accurate data exist. Moreover, the error bands are large for all the functions in the kaon and nucleon. This fact should be kept in mind for drawing any physics conclusions from experimental measurements of high-energy hadron-production processes [2].

The fragmentation functions are obtained by a global analysis of experimental data on the hadron productions [1, 3–6] in the similar way to the determination of the PDFs. Although some low moments of the PDFs can be calculated in lattice QCD, it is not possible to calculate the fragmentation functions and their moments due to a specific final state. There are some hadron models to calculate the fragmentation functions [7]; however, they are not accurate enough to calculate precise cross sections for various processes. Therefore, the global analysis of world experimental data is the most reliable way to obtain the accurate fragmentation functions. Furthermore, nuclear modifications of the fragmentation functions are also discussed recently [8] for understanding heavy-ion reactions and semi-inclusive lepton deep inelastic scattering from nuclei [9].

The fragmentation functions have been determined by several groups from analyses of experimental data on hadron productions. Until 2013, the center-of-mass (c.m.) energy of the hadron production process $e^+ + e^- \to h + X$ ranged mostly from 12 GeV to 91.2 GeV; however, many data were taken in the Z mass region of 91.2 GeV at SLD (SLAC Large Detector) and CERN-LEP (Large Electron-Positron Collider). There were lower-energy data, for example at 12, 14, 22, 29, 30, 34, 44, and 58 GeV; however, they are taken in a limited kinematical region as shown in Fig. 1 of Ref. [1]. This fact suggests that significant scaling violation should not be found in the data, which leads to large error bands in gluon fragmentation functions [1], whereas the gluon distribution function has been determined in the nucleon by scaling violation data mainly taken at HERA (Hadron-Electron Ring Accelerator).

In 2013, there were new experimental developments on the fragmentation functions in the sense that very accurate data were obtained by the Belle and BaBar collaborations for the pion and kaon [10, 11] at the energies of 10.52 GeV and 10.54 GeV, respectively. They are measured in the wide momentum-fraction region which was not covered by the previous measurements. These $e^+ + e^- \to h + X$ experiments were done at the B factories of KEK and SLAC. It is particularly important that the measurements are at a much lower energy than the Z mass because the scaling violation becomes clear in the fragmentation functions. Then, the gluon fragmentation functions should be determined more accurately. It is known that the gluon functions are very important in analyzing hadron production processes especially at RHIC (Relativistic Heavy Ion Collider) and LHC (Large Hadron Collider), where gluons play a major role in the productions. In addition, the high-statistical B-factory data should be also valuable to obtain precise quark and antiquark fragmentation functions.

These considerations made us to investigate the role of the B-factory data in the determination of the fragmentation functions because our functions are determined in 2007 without these data [1]. A purpose of this work is to show how error bands of the fragmentation functions are reduced by adding the B-factory data, as shown in Sec. 4. In addition, we discuss the details of possible flavor separation and determination of gluon function by taking

advantage of accurate measurements in the wide kinematical range between 10.5 GeV to 91.2 GeV, as explained in Sec. 3.3. The scaling violation should play an important role in determining the gluon fragmentation function.

This paper is organized as follows. In Sec. 2, hadron-production cross sections and the fragmentation functions are introduced in the e^+e^- annihilation. Then, our global analysis method is explained in Sec. 3 for determining the optimum functions, and results are discussed in Sec. 4. Finally, this work is summarized in Sec. 5.

2. Formalism

The total fragmentation function is defined by the hadron-production cross section for electron-positron annihilation ($e^+ + e^- \to h + X$) and the total hadronic cross section σ_{tot} [12]:

$$F^h(z, Q^2) = \frac{1}{\sigma_{tot}} \frac{d\sigma(e^+e^- \to hX)}{dz}. \tag{1}$$

Here, the Q^2 is given by the c.m. energy $\sqrt{s}$ as $Q^2 = s$, and the variable z is defined by the energy fraction:

$$z \equiv \frac{E_h}{\sqrt{s}/2} = \frac{2E_h}{\sqrt{Q^2}}, \tag{2}$$

where E_h and $\sqrt{s}/2$ are the hadron and beam energies, respectively. The process $e^+ + e^- \to h + X$ is described by two steps. First, a quark-antiquark pair is created by $e^+e^- \to q\bar{q}$ as shown in Fig. 1, where the intermediate state is virtual γ or Z. Therefore, the variable Q^2 is the virtual photon or Z momentum squared in $e^+e^- \to \gamma, Z$. Higher-order corrections such as $e^+e^- \to q\bar{q}g$ are taken into account in the NLO analysis. Second, a hadron h is created from quark (q), antiquark ($\bar{q}$), or gluon (g), and this process is called fragmentation. The fragmentation function approximately indicates the probability for producing a hadron, and its universality is essential for describing any hadron-production processes at high-energy reactions. The total cross section σ_{tot} in Eq. (1) is described by the $q\bar{q}$-pair creation processes, $e^+e^- \to \gamma \to q\bar{q}$ and $e^+e^- \to Z \to q\bar{q}$, with additional higher-order corrections. The explicit expression of σ_{tot} is found in Ref. [13].

A fragmentation process from a quark q is shown in Fig. 1 as an example; however, the fragmentation occurs from any primary quarks, antiquarks, and gluons. Therefore, the function

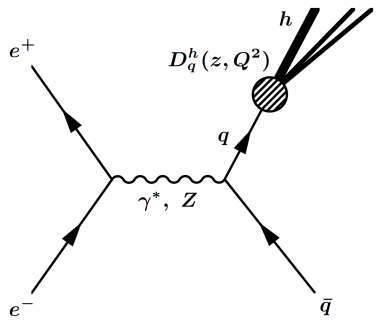

Fig. 1 Hadron production in electron-positron annihilation ($e^+ + e^- \to h + X$).

$F^h(z,Q^2)$ is expressed by the sum of their contributions:

$$F^h(z,Q^2) = \sum_i \int_z^1 \frac{dy}{y} C_i(z/y,\alpha_s)\, D_i^h(y,Q^2) \equiv \sum_i C_i(z,\alpha_s) \otimes D_i^h(z,Q^2), \tag{3}$$

where the fragmentation function of the hadron h from a parton i ($= u,\ \bar{u},\ d,\ \bar{d},\ \cdots,\ g$) is denoted as $D_i^h(z,Q^2)$, and a coefficient function is $C_i(z,\alpha_s)$ which contains perturbative QCD corrections and electroweak coupling constants. The notation $\otimes$ indicates a convolution integral defined by $f(x) \otimes g(x) = \int_x^1 dy/y f(y) g(x/y)$. Formally, the fragmentation function for the i-th quark is expressed as [14]

$$D_i^h(z) = \sum_X \int \frac{dy^-}{12\pi} e^{ik^+y^-} \mathrm{Tr}\left[\gamma^+ \left\langle 0 \left| \psi_i(0,y^-,0_\perp) \right| h,X \right\rangle \left\langle h,X \left| \bar{\psi}_i(0) \right| 0 \right\rangle\right], \tag{4}$$

where k is the parent quark momentum, and the variable z is given by the momentum ratio $z = p_h^+/k^+$ with the hadron momentum p_h. Lightcone variables are defined by $a^\pm = (a^0 \pm a^3)/\sqrt{2}$, and $\perp$ is the direction perpendicular to the third coordinate. To be precise, a gauge link is needed in Eq. (4) for the color gauge invariance. The equation indicates that a specific hadron h should be observed in the final state with the momentum fraction z. It suggests that the operator-product-expansion method cannot be applied, which is the reason why the fragmentation functions are not evaluated in lattice QCD.

The scaling violation, namely the Q^2 dependence, of the fragmentation functions (FFs) is described by the DGLAP (Dokshitzer-Gribov-Lipatov-Altarelli-Parisi) evolution equation. Its general form is the integro-differential equation [12]

$$\frac{\partial}{\partial \ln Q^2} \begin{pmatrix} D_f^h(z,Q^2) \\ D_g^h(z,Q^2) \end{pmatrix} = \frac{\alpha_s(Q^2)}{2\pi} \sum_{f'=q_j,\bar{q}_j} \begin{pmatrix} P_{f'f}(z,\alpha_s) & P_{gf}(z,\alpha_s) \\ P_{f'g}(z,\alpha_s) & P_{gg}(z,\alpha_s) \end{pmatrix} \otimes \begin{pmatrix} D_{f'}^h(z,Q^2) \\ D_g^h(z,Q^2) \end{pmatrix}, \tag{5}$$

where f indicates $f = q_i, \bar{q}_i$, N_f is the number of quark flavors, $\alpha_s(Q^2)$ is the running coupling constant of QCD, and the function $P_{ij}(z)$ is time-like splitting function. One notices that i and j are interchanged from the space-like DGLAP equations for the PDFs. In addition, it should be noted that the time-like splitting functions are generally different from the space-like ones if higher-order perturbative corrections are taken into account [12, 15, 16]. The actual expressions of $P_{ij}(z)$ are lengthy in the NLO (next-to-leading-order) of α_s, so that they should be found, for example, in Ref. [12].

The evolution equations are complicated integro-differential equations especially if higher-order α_s corrections are included. Therefore, they cannot be solved in analytical methods. Various numerical methods have been developed and their references should be found in Refs. [17, 18]. In the work of Ref. [18], the equations are solved by using the Gauss-Legendre quadrature for evaluating integrals, and a useful code is provided for calculating the Q^2 evolution of the fragmentation functions in the leading order (LO) and NLO of α_s. The renormalization scheme is the modified minimal subtraction ($\overline{\mathrm{MS}}$) scheme in the NLO evolution. We use this Q^2 evolution code in our global analysis of this article.

3. Analysis method

3.1. Initial fragmentation functions

The FFs are determined by global analyses of world data on hadron-production processes. They are parametrized in a simple polynomial form of z at a fixed Q^2 which is denoted as

Q_0^2. Because it is the purpose of this work to show modifications of uncertainties in the FFs from the previous analysis without the B-factory data [1], we use the same function

$$D_i^h(z, Q_0^2) = N_i^h z^{\alpha_i^h} (1-z)^{\beta_i^h}, \tag{6}$$

where N_i^h, α_i^h, and β_i^h are parameters to be determined by the global analysis. A more complicated functional form is usually employed in the PDF analysis; however, the data variety is enough to probe minute z dependence in the FF case. In our analysis, the initial scale Q_0^2 is taken as $Q_0^2 = 1$ GeV^2 for gluon and light quarks (u, d, s), and it is taken at the masses m_c^2 and m_b^2 for charm and bottom quark FFs.

The second moments of the FFs are defined by

$$M_i^h = \int_0^1 dz\, z\, D_i^h(z, Q^2), \tag{7}$$

and they are related to the overall constants N_i^h with the beta function as $N_i^h = M_i^h / B(\alpha_i^h + 2, \beta_i^h + 1)$. Since there is a sum rule for the second moments: $\sum_h M_i^h = 1$, it is more appropriate to use the parameter set (M_i^h, α_i^h, β_i^h) in the global analysis, rather than the set (N_i^h, α_i^h, β_i^h) in order to exclude an unphysical solution with a sum which significantly exceeds one even by the summation over $h = \pi$ and K.

In general, different parameters are assigned for favored and disfavored FFs, separately. The favored means the fragmentation from a quark which exits in the hadron h as a constituent in the naive SU(6) quark model, whereas the disfavored means the fragmentation from a sea quark. Although it is known that light sea-quark (up, down, strange sea quarks) distributions are not flavor symmetric in the unpolarized PDFs [19], they are assumed to be the same in the present analysis of the FFs.

Considering the basic quark configuration in the pion ($\pi^+(u\bar{d})$), we assign the same functions for the favored functions of u and $\bar{d}$:

$$D_u^{\pi^+}(z, Q_0^2) = D_{\bar{d}}^{\pi^+}(z, Q_0^2). \tag{8}$$

On the other hand, the disfavored functions of π^+ are assumed to be equal in the initial scale:

$$D_{\bar{u}}^{\pi^+}(z, Q_0^2) = D_d^{\pi^+}(z, Q_0^2) = D_s^{\pi^+}(z, Q_0^2) = D_{\bar{s}}^{\pi^+}(z, Q_0^2). \tag{9}$$

In addition, we have separate gluon, charm-quark, and bottom-quark FFs:

$$D_g^h(z, Q_0^2), \quad D_c^h(z, m_c^2) = D_{\bar{c}}^h(z, m_c^2), \quad D_b^h(z, m_b^2) = D_{\bar{b}}^h(z, m_b^2), \tag{10}$$

where $h = \pi^+$ or K^+ in the following kaon parametrization. In analyzing the pion data of the e^+e^- annihilation, the charged-pion combination ($\pi^+ + \pi^-$) data are analyzed. The FFs of π^- are obtained from the π^+ ones by using the charge symmetry at any Q^2 which is not necessarily Q_0^2 as long as Q^2 is in the perturbative QCD region:

$$D_q^{\bar{h}}(z, Q^2) = D_{\bar{q}}^h(z, Q^2), \quad D_g^{\bar{h}}(z, Q^2) = D_g^h(z, Q^2). \tag{11}$$

The FFs of the kaon are taken in the same way by considering the constituent-quark configuration $K^+(u\bar{s})$; however, the antistrange function is taken differently from the up-quark function in the favored FFs:

$$D_u^{K^+}(z, Q_0^2), \quad D_{\bar{s}}^{K^+}(z, Q_0^2). \tag{12}$$

The disfavored functions are taken as the same:

$$D_{\bar{u}}^{K^+}(z,Q_0^2) = D_d^{K^+}(z,Q_0^2) = D_{\bar{d}}^{K^+}(z,Q_0^2) = D_s^{K^+}(z,Q_0^2). \tag{13}$$

There are also gluon, charm-quark, and bottom-quark FFs as given in Eq. (10). For K^-, the relations of Eq. (11) are used to obtain the functions from the ones of K^+.

3.2. Experimental data

The fragmentation functions are determined by global analyses of charged-hadron production data of $e^+ + e^- \to h^\pm + X$, where the hadron $h^\pm$ is charged pion ($\pi^+ + \pi^-$) or charged kaon ($K^+ + K^-$) in this work. We use the data from the measurements of TASSO [20–22], TPC [23], HRS [24], TOPAZ [25], SLD [26], ALEPH [27], OPAL [28], and DELPHI [29, 30] as they are employed in the analysis of 2007 [1]. In addition, we include the new Belle [10] and BaBar [11] data in our analyses of pion and kaon. Experimental collaborations, laboratories, references, center-of-mass (c.m.) energies, and numbers of the data are listed in Table 1 [31].

The kinematical cuts, $Q^2 > 1$ GeV^2, $z > 0.1$ ($z > 0.15$) for the data at $\sqrt{s} < M_Z$ (BaBar kaon), and $z > 0.05$ for the data at $\sqrt{s} = M_Z$, are applied in using the measured data. The perturbative QCD is used in obtaining the coefficient functions and splitting functions in Eqs. (3) and (5), respectively. $Q^2 > 1$ GeV^2 is considered to be region where the perturbative QCD can be applied. The z-cut condition is applied because of resummation of soft-gluon logarithms [32]. The resummation effects need to be properly handled in the formalism for describing the small-z data, whereas a fixed-order formalism is used in this work. We applied the z cut for the BaBar data at $z > 0.15$ because the total fragmentation function decreases steeply at small z, where the modified leading logarithm approximation (MLLA) is needed

Table 1 Experimental collaborations, laboratories, references, center-of-mass energies, and numbers of data points are listed for used data sets of $e^+ + e^- \to \pi^\pm + X$, $K^\pm + X$ [31]. TASSO $\sqrt{s} = 44$ GeV data exist only for $\pi^\pm$.

Experiment	Lab.	Ref.	$\sqrt{s}$	# of π data	# of K data
Belle	KEK	[10]	10.52	78	78
BaBar	SLAC	[11]	10.54	36	36
TASSO	DESY	[20–22]	12,14,22,30,34,(44)	29	18
TPC	SLAC	[23]	29	18	17
HRS	SLAC	[24]	29	2	3
TOPAZ	KEK	[25]	58	4	3
SLD	SLAC	[26]	91.28	29	29
SLD (u,d,s)	SLAC	[26]	91.28	29	29
SLD (c)	SLAC	[26]	91.28	29	29
SLD (b)	SLAC	[26]	91.28	29	28
ALEPH	CERN	[27]	91.2	22	18
OPAL	CERN	[28]	91.2	22	10
DELPHI	CERN	[29]	91.2	17	27
DELPHI (u,d,s)	CERN	[29]	91.2	17	17
DELPHI (b)	CERN	[29]	91.2	17	17
total				378	359

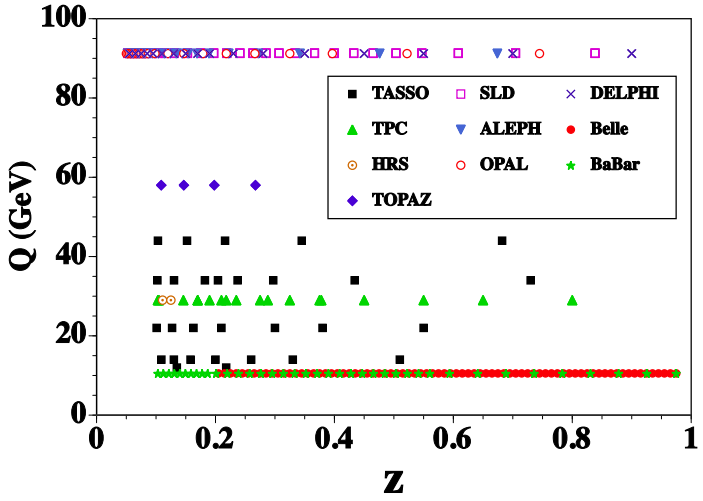

Fig. 2 Kinematical range is shown by z and $Q(=\sqrt{s})$ values for the pion data. The Belle and BaBar data are shown by the filled circles and asterisks at $Q \simeq 10.5$ GeV, respectively.

for theoretically describing such behavior [11, 32]. In addition, the BaBar multiplicities are shown by the momentum fraction x_p, and the MLLA-necessity region could shift to larger z ($\approx 0.10 - 0.15$) if the finite kaon mass is used in converting x_p to z. Since we use the fixed-order formalism in analyzing the data, these small-z cut conditions are applied.

The kinematical region of the pion data is shown in Fig. 2. In comparison with the previous analysis [1], the additional data are from the Belle and BaBar measurements, which are shown by the filled circles and asterisks at $Q = 10.52$ GeV and 10.54 GeV. It is obvious that these B-factory data significantly extend the kinematical region at small Q^2 at large z. As one notices from the figure, many previous data are taken especially at the Z mass M_Z. There are not so many data in the lower-energy region except for the Belle and BaBar. The kaon data of the Belle and BaBar collaborations are taken in the same kinematical region.

The B-factory data are taken at 10.5 GeV. In comparison with the data at M_Z, the scaling violation should become clearer for the first time in the fragmentation functions. Since the scaling violation is used for determining the gluon distribution in the PDFs, it became realistic to determine the gluon fragmentation functions by the B-factory data in combination with others. In using the Belle data, one needs to be careful about the correction factor due to the initial-state radiation (ISR). Because of the ISR, the energy scale $\sqrt{s}/2$ is modified and the measurements contain the variation of this scale. The Belle data are supplied by applying a cut for the energy variation $E_{\rm ISR} < 0.5\%\sqrt{s}/2$, namely $(d\sigma^h/dz)_{E_{\rm ISR}<0.5\%\sqrt{s}/2} = c \cdot d\sigma^h/dz$, where c is the normalization correction factor due to the kinematical cut. Therefore, if the total cross section is estimated by the Belle data in a global analysis, the total fragmentation function should be given by

$$F^h = \frac{1}{(\sigma_{tot})_{E_{\rm ISR}<0.5\%\frac{\sqrt{s}}{2}}} \left(\frac{d\sigma_{e^+e^-\to hX}}{dz}\right)_{E_{\rm ISR}<0.5\%\frac{\sqrt{s}}{2}} = \frac{1}{c\,\sigma_{tot}} \left(\frac{d\sigma_{e^+e^-\to hX}}{dz}\right)_{\rm Belle\ data}, \quad (14)$$

where the total cross section σ_{tot} is calculated theoretically. The correction factor c is estimated by the Monte-Carlo simulation by the Belle collaboration. It could be approximated by an z-independent constant, and it is given by $c = 0.64616 \pm 0.00003$ [10].

The BaBar measurements are provided by two types of data: conventional and prompt. The prompt hadron data include primary hadrons or decay products from particles with lifetimes shorter than 10^{-11}s. This set does not include the decays of hadron with lifetimes in the range $1-3\times10^{-11}$s, such as weakly decaying baryons and K^0_S. These decays are added to the prompt data and the resulting data set is called the conventional one. Most other measurements include all the decays, so that the conventional set is close to the other publications obtained by similar data handling. In our work, the conventional set is used; however, we find that the prompt set is numerically more consistent with previous measurements of the LEP and SLD. In comparison with the Belle pion data, we find that the Belle measurements are between the BaBar prompt and conventional data sets. The Belle pion data are larger than the BaBar prompt in the total fragmentation function of Eq. (1), so that a large normalization correction is needed for the Belle if the BaBar prompt data are included in the global analysis. Since there is no such significant difference between the prompt and conventional sets in the kaon, the normalization shifts for both Belle and BaBar data are not large as we show in Sec. 4.

3.3. Flavor separation and determination of gluon fragmentation function

The total FF measured in e^+e^- annihilation is given in Eqs.(1) and (3). Since the contribution from a quark and its antiquark is equal, the cross section is given by the "plus-component"of the quark FFs, $D_{q_i^+}\equiv D_{q_i}+D_{\bar{q}_i}$, and the gluon FF D_g. In the global analysis, the heavy-flavor FFs are mainly determined from the flavor-tagged data [26, 30], while separation of the light-flavor FFs is possible due to the charge difference between the electromagnetic and weak interactions and also due to the effects of the scale evolution with a help of some plausible assumptions for the favored and disfavored FFs at the initial scale. The gluon FF is determined mainly through the scale evolution.

To illustrate these points, let us consider the pure-QED process at $Q^2\ll M_z^2$, where the intermediate Z boson can be neglected. For simplicity, we take the number of flavor $N_f=3$ in the following discussion or we consider the cross sections by subtracting the heavy-quark contributions. In any case, the charm and bottom functions could be determined separately by the c- and b-tagged data in Table 1. The total FF in this case is expressed up to the NLO as

$$F^h(z,Q^2)=C_u(z)\otimes\left[D_{u^+}(z,Q^2)+\frac{1}{4}D_{d^+}(z,Q^2)+\frac{1}{4}D_{s^+}(z,Q^2)\right]+C_g(z)\otimes D_g(z,Q^2), \quad (15)$$

where C_u and C_g denote the coefficient functions for u-quark and gluon, respectively. We note that the quark coefficient functions include the charge-factor squared e_q^2. The gluon coefficient function is order α_s suppressed, so that the quark FFs are primarily determined from the e^+e^- annihilation data. The evolution equations for those FFs are obtained from (5) as

$$\begin{aligned}\frac{\partial}{\partial\ln Q^2}D_{q_i^+}(z,Q^2)&=\bar{\alpha}_sP^+_{NS}(z)\otimes D_{q_i^+}(z,Q^2)+\bar{\alpha}_sP_{PS}(z)\otimes D_\Sigma(z,Q^2)\\&\quad+2\,\bar{\alpha}_sP_{gq}(z)\otimes D_g(z,Q^2), \quad (16)\\ \frac{\partial}{\partial\ln Q^2}D_g(z,Q^2)&=\bar{\alpha}_sP_{qg}(z)\otimes D_\Sigma(z,Q^2)+\bar{\alpha}_sP_{gg}(z)\otimes D_g(z,Q^2), \quad (17)\end{aligned}$$

where $\bar{\alpha}_s \equiv \alpha_s/(2\pi)$ and $D_\Sigma \equiv \sum_i^{N_f} D_{q_i^+}$. Here, we have performed the standard decompositions for the splitting functions into flavor singlet (S) and nonsinglet (V) terms [12]

$$P_{q_iq_j} = \delta_{ij}P^V_{qq} + P^S_{qq}\,, \quad P_{q_i\bar{q}_j} = \delta_{ij}P^V_{q\bar{q}} + P^S_{q\bar{q}}\,, \tag{18}$$

and we defined the nonsinglet (NS) and pure-singlet (PS) components of the qq-type splitting functions as

$$P_{q_iq_j} + P_{q_i\bar{q}_j} = \delta_{ij}\left(P^V_{qq} + P^V_{q\bar{q}}\right) + P^S_{qq} + P^S_{q\bar{q}} \equiv \delta_{ij}P^+_{NS} + P_{PS}\,. \tag{19}$$

Similarly, the scale evolution of the "minus" component of the quark FF, $D_{q_i^-} \equiv D_{q_i} - D_{\bar{q}_i}$, is governed by

$$\frac{\partial}{\partial \ln Q^2} D_{q_i^-}(z,Q^2) = \bar{\alpha}_s P^-_{NS}(z) \otimes D_{q_i^-}(z,Q^2)\ , \tag{20}$$

with the splitting function: $P^-_{NS} \equiv P^V_{qq} - P^V_{q\bar{q}}$.

The solution of the evolution equation can be expressed concisely in terms of the evolution functions [33]. For example, the solution of Eq.(20) is expressed as

$$D_{q_i^-}(z,Q^2) = E^-_{NS}(z;\,Q^2,Q_0^2) \otimes D_{q_i^-}(z,Q_0^2), \tag{21}$$

where the evolution function $E^-_{NS}(z;Q^2,Q_0^2)$ is given in terms of the splitting functions P^-_{NS} and QCD beta function. The solutions for the singlet FFs are also expressed in a matrix form with the evolution functions given by the singlet splitting functions. Substituting the solution for each flavor component, we rewrite the total FF as

$$\begin{aligned} F^h(z,Q^2) = C_u(z) \otimes \Bigg[& E^+_{NS}(z;\,Q^2,Q_0^2) \otimes \left\{ \frac{1}{2}D_{u^+}(z,Q_0^2) - \frac{1}{4}D_{d^+}(z,Q_0^2) - \frac{1}{4}D_{s^+}(z,Q_0^2) \right\} \\ & + \frac{1}{2}\left\{ E_{\Sigma\Sigma}\left(z;\,Q^2,Q_0^2\right) \otimes D_\Sigma(z,Q_0^2) + E_{g\Sigma}\left(z;\,Q^2,Q_0^2\right) \otimes D_g(z,Q_0^2) \right\} \Bigg] \\ & + C_g(z) \otimes \left[E_{qg}(z;\,Q^2,Q_0^2) \otimes D_\Sigma(z,Q_0^2) + E_{gg}\left(z;\,Q^2,Q_0^2\right) \otimes D_g(z,Q_0^2) \right], \end{aligned} \tag{22}$$

where $E_{\Sigma\Sigma}$, $E_{g\Sigma}$, E_{qg}, and E_{gg} are given by the splitting functions $P^+_{NS} + n_f P_{PS}$, $2n_f P_{gq}$, P_{qg}, and P_{gg}, respectively, with the number of flavor n_f. In Eq.(22), three independent sets of FFs at the initial scale, namely, $D_{u^+}(z,Q_0^2)$, $D_{d^+}(z,Q_0^2) + D_{s^+}(z,Q_0^2)$ and $D_g(z,Q_0^2)$ appear with different combinations of the evolution functions. The first two sets of FFs give the dominant contribution because of the relations: $C_u/e_u^2 = \delta(1-z) + \mathcal{O}(\alpha_s)$, $C_g = \mathcal{O}(\alpha_s)$; $E_{NS}, E_{\Sigma\Sigma}, E_{gg} = \delta(1-z) + \mathcal{O}(\alpha_s \ln(Q^2/Q_0^2))$; $E_{qg}, E_{g\Sigma} = \mathcal{O}(\alpha_s \ln(Q^2/Q_0^2))$. The relative weights of these three sets change as the scale Q^2 evolves, so that these sets can be separated from each other in principle. However, if we only rely on the pure-QED process with the intermediate γ, a clear separation of these sets requires high precision data at least at three distinct energies.

In the case of the e^+e^- annihilation at the Z pole, the total FF is given by

$$\begin{aligned} F^h(z,M_Z^2) = \tilde{C}_q(z) \otimes \Big[& (c_V^{u\,2} + c_A^{u\,2})\big\{ D_{u^+}(z,M_Z^2) + D_{c^+}(z,M_Z^2) \big\} \\ & + (c_V^{d\,2} + c_A^{d\,2})\big\{ D_{d^+}(z,M_Z^2) + D_{s^+}(z,M_Z^2) + D_{b^+}(z,M_Z^2) \big\} \Big] + C_g(z) \otimes D_g(z,M_Z^2). \end{aligned} \tag{23}$$

Here, $\tilde{C}_q$ is given by replacing the quark-charge square e_q^2 within C_q of Eq. (22) by weak couplings and then taking the couplings $c_V^{q\,2} + c_A^{q\,2}$ out from the coefficient function. The vector and axial-vector couplings are given by $c_V^q = T_q^3 - 2e_q \sin^2\theta_W$ and $c_A^q = T_q^3$, respectively

[34]. Taking $\sin^2\theta_W = 0.23$ [35], we have $c_V^{u\,2} + c_A^{u\,2} = 0.287$ and $c_V^{d\,2} + c_A^{d\,2} = 0.370$, which are roughly the same. Therefore, we have

$$\begin{aligned} F^h(z, M_Z^2) &\approx \tilde{C}'_q(z) \otimes D_\Sigma(z, M_Z^2) + C_g(z) \otimes D_g(z, M_Z^2) \\ &= \tilde{C}'_q(z) \otimes \left[E_{\Sigma\Sigma}(z; M_Z^2, Q_0^2) \otimes D_\Sigma(z, Q_0^2) + E_{g\Sigma}(z; M_Z^2, Q_0^2) \otimes D_g(z, Q_0^2) \right] \\ &\quad + C_g(z) \otimes \left[E_{qg}(z; M_Z^2, Q_0^2) \otimes D_\Sigma(z, Q_0^2) + E_{gg}(z; M_Z^2, Q_0^2) \otimes D_g(z, Q_0^2) \right], \end{aligned} \tag{24}$$

where $\tilde{C}'_q = 0.33\,\tilde{C}_q$, which is approximately the average of $0.287\,\tilde{C}_q$ and $0.370\,\tilde{C}_q$, and the dominant contribution comes only from the singlet quark FF.

Now, we discuss separation of the quark flavors and determination of the gluon FF by using the e^+e^- annihilation data both at and below the Z-pole. Note that in Eqs. (22) and (24), (or (23) to be precise), D_{u^+} and $D_{d^+} + D_{s^+}$ appear as the dominant contributions with different relative weights, due to the difference of the electric and weak charges of quarks. Therefore, even if we ignore the evolution effects, those two sets of FFs can be separately determined in a relatively clear manner. The impact of the B-factory data is understood as follows.

(1) In the global fit before the B-factory data, the e^+e^- annihilation data have been dominated by the LEP and SLD data, from which the singlet FF is mainly determined.
(2) Then, by combining with the pure-QED process data at lower energies with a moderate precision, the two components of the quark FFs, $D_{u^+}(Q_0^2)$ and $D_{d^+}(Q_0^2) + D_{s^+}(Q_0^2)$ can be separated as mentioned above.
(3) On the other hand, determination of the gluon FF, especially its separation from the singlet FF must rely on changes of their relative weights through the scale evolution, so that the precise determination of the gluon FF requires high precision data at energy scales much lower than the Z mass. The B-factory data are considered to provide such information.

So far, we have discussed flavor separation and determination of the gluon FF based on the cross section formula and the scaling violation. Now, we introduce the favored and disfavored FFs (D_{fav}, D_{dis}) at the initial scale. Let us take the pion case, where we have the initial relations at Q_0^2:

$$D_{u^\pm}^{\pi^+}(z, Q_0^2) = \pm D_{d^\pm}^{\pi^+}(z, Q_0^2),\ D_{s^-}^{\pi^+}(z, Q_0^2) = 0,\ D_{u^+}^{\pi^+}(z, Q_0^2) - D_{u^-}^{\pi^+}(z, Q_0^2) = D_{s^+}^{\pi^+}(z, Q_0^2), \tag{25}$$

which are equivalent to Eqs. (8) and (9). From Eqs. (16) and (20), one can see that the first two relations are preserved, whereas the third relation is violated by the scale evolution to $Q^2 \neq Q_0^2$. This assignment of favored and disfavored FFs assumes the constituent quark model, the OZI (Okubo-Zweig-Iizuka) rule, and the flavor $SU(3)$ symmetry in fragmentation process at the initial scale Q_0^2. In the actual fitting procedure, this assignment is nothing but a change of the independent sets of the initial FFs:

$$\begin{aligned} D_{u^+}^{\pi^+}(z, Q_0^2) &\to D_{fav}^{\pi^+}(z, Q_0^2) + D_{dis}^{\pi^+}(z, Q_0^2), \\ D_{d^+}^{\pi^+}(z, Q_0^2) + D_{s^+}^{\pi^+}(z, Q_0^2) &\to D_{fav}^{\pi^+}(z, Q_0^2) + 3D_{dis}^{\pi^+}(z, Q_0^2), \end{aligned} \tag{26}$$

in Eqs. (22) and (23). Therefore, $D_{fav}^{\pi^+}$ and $D_{dis}^{\pi^+}$ can be well-determined separately by using the LEP and SLD data and the pure-QED process data as discussed above. Instead, one can also use a more general parametrization without assuming the third relation in Eq.

(25), by taking $D_{u,\bar{d}}(Q_0^2) = D_{fav}^{\pi^+}(Q_0^2)$, $D_{\bar{u},d}(Q_0^2) = D_{dis(1)}^{\pi^+}(Q_0^2)$ and $D_{s,\bar{s}}^{\pi^+}(Q_0^2) = \tilde{D}_{dis(2)}^{\pi^+}(Q_0^2)$. Advantages of this parametrization are that it takes the $SU(3)$ breaking effect in the fragmentation process and is compatible with the scale evolution. However, since the separation of these three sets of FFs must rely on the scale evolution, it is as hard as the determination of the gluon FF.

For the kaon, we have the initial relations:

$$\begin{aligned} &D_{d^-}^{K^+}(z,Q_0^2) = 0 \ , \\ &D_{d^+}^{K^+}(z,Q_0^2) = D_{u^+}^{K^+}(z,Q_0^2) - D_{u^-}^{K^+}(z,Q_0^2) = D_{s^+}^{K^+}(z,Q_0^2) - D_{s^-}^{K^+}(z,Q_0^2) \ , \end{aligned} \tag{27}$$

where the first relation is preserved, while the second and third ones are violated by the scale evolution. The flavor separation in the kaon case is similar to the one in the case we have just discussed above as a generalized parametrization for pion. It is not easy to determine two favored functions $D_u^{K^+}$ and $D_{\bar{s}}^{K^+}$, one disfavored function $D_{dis}^{K^+}$, and the gluon function $D_g^{K^+}$ simultaneously in comparison with the one favored function for the pion.

To summarize, flavor separation of two sets of quark FFs can be done clearly by using the e^+e^- annihilation at and below the Z-pole, which is due to the difference of the quark coupling to the virtual photon and Z. On the other hand, flavor separation of three sets of quark FFs and determination of the gluon FF requires the effects of the scaling evolution. The data from B-factory measurements, obtained at an energy much lower than the Z mass with a wide z range, are expected to provide a major assistance for the latter analyses. Specifically, the uncertainty of the gluon FF is expected to decrease significantly once the B-factory data are included in the analysis and provided that the quark FFs have been determined with enough accuracy without the B-factory data.

3.4. χ^2 analysis

As shown in Fig. 2, the experimental data are taken at various Q^2 values, which are different from the initial scale $Q_0^2 = 1$ GeV^2. The timelike DGLAP equation (5) is used for calculating the Q^2 evolution. The scale parameter is taken $\Lambda_{NLO}^{(4)}$=0.323 GeV for four flavors [36]. This value is changed with the number of flavors at the heavy-quark thresholds, and it is $\alpha_s(M_z) = 0.119$ at the Z mass. The charm and bottom quark masses are $m_c = 1.43$ GeV and $m_b = 4.3$ GeV in our analyses. These values are the same in the previous analysis [1], and the $\overline{\rm MS}$ scheme is used in the NLO. The numerical solution is calculated by the method of Ref. [18] for the Q^2 evolution. The initial functions are evolved to the experimental points of Q^2. Then, the theoretical fragmentation function F_j^{theo} is calculated by Eq. (3) at the experimental Q^2 point to compare it with the experimental one F_j^{data} in Eq. (1).

The total χ^2 is then given by [37]

$$\chi^2 = \sum_{i=1}^{n} \left[\sum_{j=1}^{m} \frac{(D_j - T_j/N_i)^2}{(\sigma_j^{\rm exp})^2} + \frac{(N_i - 1)^2}{\sigma_{N_i}^2} \right] \tag{28}$$

where T_j and D_j are theoretical calculation and a datum, respectively, and N_i (σ_{N_i}) is the normalization factor (its error) for the data set i. For simplification of discussions about consistency of the B-factory data sets with other measurements, the overall normalization factors are introduced. Correlations of the systematic errors are not considered, and the experimental errors are calculated from systematic and statistical errors by $(\sigma_j^{\rm exp})^2 = (\sigma_j^{\rm stat})^2 + (\sigma_j^{\rm sys})^2$.

As the overall scale shifts on the data, the free factors are used only for the B-factory data sets. Its values for the other data sets are fixed as $N_i = 1$. The optimum parameters are obtained by minimizing χ^2 by the CERN subroutine `MINUIT` [38]. Uncertainties of the PDFs have been calculated, for example, as explained in Refs. [39, 40]. Here, the Hessian method is employed to calculate the uncertainties of the FFs .

We denote the parameters of the FFs as ξ_i (i=1, 2, $\cdots$, N). The total χ^2 is expanded around the minimum point $\hat{\xi}$ by keeping only the quadratic term:

$$\Delta\chi^2(\xi) = \chi^2(\hat{\xi} + \delta\xi) - \chi^2(\hat{\xi}) = \sum_{j,k} H_{jk}\, \delta\xi_j\, \delta\xi_k \ , \tag{29}$$

where H_{jk} is called Hessian. The errors of the FFs are estimated by supplying the value of $\Delta\chi^2$, which determines the confidence level. Using the Hessian matrix, which is numerically obtained by running the `MINUIT` code, we calculated the errors of the FFs by

$$[\delta D_i^h(z)]^2 = \Delta\chi^2 \sum_{j,k} \left(\frac{\partial D_i^h(z,\xi)}{\partial \xi_j}\right)_{\hat{\xi}} H_{jk}^{-1} \left(\frac{\partial D_i^h(z,\xi)}{\partial \xi_k}\right)_{\hat{\xi}} . \tag{30}$$

We note that the Hessian method assumes that the quadratic expansion of Eq. (29) would give a good approximation of χ^2 in the vicinity of the minimum. A detailed study employing the Lagrange multiplier technique suggests that this assumption is indeed feasible in most cases [6].

As well known, $\Delta\chi^2 = 1$ gives the confidence level of 68%, namely the one-σ-error range, if the number of parameter is one. For the multiparameters with N degrees of freedom, the confidence level could be calculated by

$$P = \int_0^{\Delta\chi^2} \frac{1}{2\ \Gamma(N/2)} \left(\frac{S}{2}\right)^{\frac{N}{2}-1} \exp\left(-\frac{S}{2}\right) dS \ , \tag{31}$$

as explained in Ref. [41]. As a $\Delta\chi^2$ criterion, we applied this one-σ range for the probability distribution in the multi-parameter space. We use the $\Delta\chi^2$ value to obtain the one-σ-error range $P = 0.6826$ by Eq. (31). It is given by $\Delta\chi^2 = 15.94$ for $N = 14$ in the pion analysis and $\Delta\chi^2 = 19.20$ for $N = 17$ in the kaon. Roughly, these values correspond to $\Delta\chi^2 \sim N$. One may note that if a physical value is calculated by the determined fragmentation functions with multi-parameters, it could be statistically right to show the one-σ range by $\Delta\chi^2 = 1$. Our choice of $\Delta\chi^2 \sim N$ could be considered as a tolerance value in the unpolarized PDF analysis. In the PDF studies, different values are used for $\Delta\chi^2$ depending on analysis groups. More details are explained in Ref. [40] for the polarized PDFs, the interested reader may look at this article.

4. Results

Analysis results are shown by χ^2 values for all the used experimental data sets of the pion and kaon in Table 2. Here, the values in the parentheses are χ^2 values of the HKNS07 NLO analysis [1] without the B-factory data. In the pion analyses, the Belle and BaBar χ^2 values in the table consist of the first (data) and second (normalization) terms in Eq. (28), and they are 44.3=24.1 (1st)+20.2 (2nd) for the Belle and 141.6=44.9 (1st)+96.7 (2nd) for the BaBar. We notice that the normalization contributions to the total χ^2 are large. The first χ^2 value of the Belle is very small by considering the number of data of 78, whereas the agreement

Table 2 Each χ^2 contribution in the pion and kaon NLO analysis. The normalization factors are also shown for Belle and BaBar. The values in the parentheses ( ) indicate the ones of the HKNS07 parametrization [1] without the Belle and BaBar data.

experiment	# of π data	$\chi^2(\pi)$	$N_i(\pi)$	# of K data	χ^2(K)	N_i(K)
Belle	78	44.3 (–)	0.94	78	18.8 (–)	1.03
BaBar	36	141.6 (–)	0.90	36	37.8 (–)	0.96
TASSO	29	55.2 (51.9)	–	18	26.2 (25.0)	–
TPC	18	14.2 (27.3)	–	17	40.5 (15.2)	–
HRS	2	4.1 (2.0)	–	3	0.4 (0.4)	–
TOPAZ	4	3.9 (2.6)	–	3	1.7 (0.8)	–
SLD (all)	29	41.7 (10.6)	–	29	17.0 (12.3)	–
SLD (u,d,s)	29	90.7 (36.4)	–	29	59.3 (57.2)	–
SLD (c)	29	36.0 (26.1)	–	29	39.3 (32.4)	–
SLD (b)	29	67.7 (66.4)	–	28	99.0 (88.7)	–
ALEPH	22	47.5 (24.0)	–	18	8.7 (12.8)	–
OPAL	22	57.1 (45.8)	–	10	9.1 (11.5)	–
DELPHI (all)	17	37.2 (48.6)	–	27	15.0 (15.2)	–
DELPHI (u,d,s)	17	24.8 (31.1)	–	17	23.0 (22.1)	–
DELPHI (b)	17	64.4 (60.8)	–	17	10.1 (11.7)	–
total	378 (264)	730.4 (433.5)		359 (245)	405.9 (305.1)	
total/d.o.f.		2.02 (1.73)			1.19 (1.34)	

with the BaBar data is marginal. However, the normalization shifts are significantly larger than experimental estimations for the overall normalization errors, 1.4% (0.98%) for Belle (BaBar). It indicates that the B-factory measurements are not completely consistent with the previous data. We notice in the table that the χ^2 values become larger than the previous HKNS07 ones for the SLD measurements except for the bottom-quark data, whereas the χ^2 values stay almost the same for the TASSO, OPAL, and DELPHI.

Actual comparisons of the NLO pion results with the data are shown in Fig. 3, where the fractional differences, (Data−Theory)/Theory, are shown for all the data sets. As suggested by the small χ^2 for the Belle data in Table 2, the agreement with the Belle data is very good in the top figure ($Q = 10.5$ GeV) of Fig. 3. It is also clear that the Belle and BaBar data have excellent accuracies in comparison with the other ones. Because of the tiny errors of the B-factory data, the parametrized functions converge so as to fit these data as shown in the top figure of Fig. 3. It results into deviations from some data sets. There are noticeable differences from the SLD data although their errors are small, which makes large χ^2 contributions as noticed in Table 2 and suggests that there are some discrepancies between the B-factories and SLD ones. On the other hand, the LEP (OPAL, DELPHI) data have good agreement with the obtained theoretical functions although there are slight differences from the LEP-ALEPH data.

The determined FFs of the pion (π^+) are shown for the NLO in Fig. 4. In order to show the improvements due to the B-factory data, the FFs and their uncertainties of the previous version HKNS07 are shown for comparison in Fig. 4 (a). We find that the gluon and

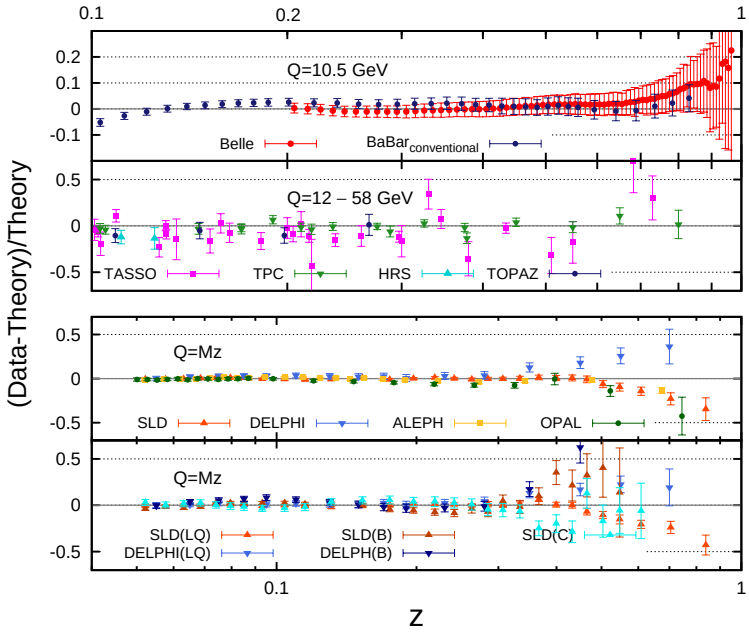

Fig. 3 Comparison of theoretical results at the NLO with charged-pion production data. The z scale ranges from 0.1 to 1 in the upper two figures (Belle, BaBar; TASSO, TPC, HRS, TOPAZ), and it is from 0.04 to 1 in the lower two figures (SLD, DELPHI, ALEPH, OPAL; SLD(LQ,B,C), DELPHI(LQ,B)).

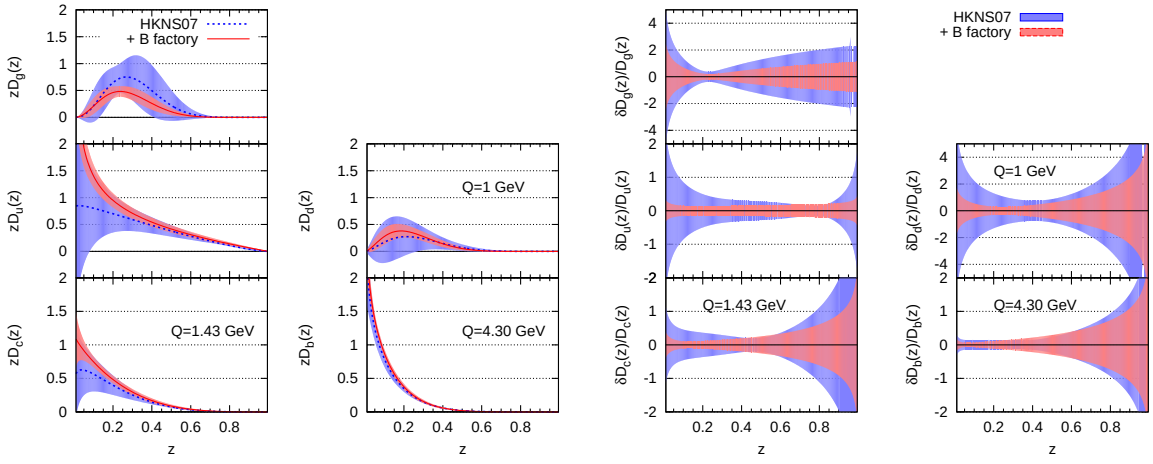

(*a*) (*b*)

Fig. 4 (*a*) Fragmentation functions and their uncertainties are shown for π^+ at Q^2=1 GeV^2, m_c^2, and m_b^2 in the NLO analysis. (*b*) Relative uncertainties are shown. The dashed and solid curves indicate HKNS07 and current (HKKS16) results, and the HKNS07 and HKKS16 uncertainties are shown by the dark- and light-shaded bands, respectively.

light-quark FFs are changed from the HKNS07 ones. Especially, the favored fragmentation function $D_u^{\pi^+}$ increases steeply at small z as shown in this figure, and it is the cause of the χ^2 increase for SLD. Moreover, the second moment of $D_u^{\pi^+}$ becomes larger than the HKNS07 one, and it reaches almost the upper limit of the momentum sum for the current analysis. It could suggest that a more flexible functional form is required for the favored FF in order to keep the sum rule. However, even if the flexible form is introduced, it seems to be difficult to explain the SLD data because they cannot be fit at the same time with the B-factory and DELPHI data because of their inconsistencies in Fig. 3.

There are significant reductions of the uncertainty bands in all the FFs. There are two sources of these reductions due to the B-factory data. First, the precise data at $\sqrt{s} \simeq 10.5$ GeV combined with other accurate data taken at larger Q^2, mainly at $Q^2 = M_Z^2$, make it possible to determine the quark FFs precisely. It is apparently shown by the smaller errors in the favored and disfavored quark FFs. This is due to the fact that the quark-pair production is dominated by the electro- and weak-interaction in the B-factory and LEP/SLD data, respectively, so that $F^{\pi^\pm}$ is given by D_{fav} and D_{dis} with different relative weights in Eqs. (22) and (23). Second, the scaling violation information between the B-factory and $Q^2 = M_Z^2$ data should impose a constraint on the gluon FF. In fact, the gluon fragmentation function is determined more accurately by including the B-factory data. Furthermore, if the gluon function is obtained more accurately, it affects the better determination of the quark FFs due to error correlation effects. Thus, these results for the pion FFs are consistent with the discussion given in Sec. 3.3.

Kaon data are also analyzed by including the new B-factory data. First, the χ^2 values are shown in Table 2. In the pion case, there are some differences in the χ^2 values of the HKNS07 data sets with or without the B-factory ones; however, the χ^2 values stay almost the same as the HKNS07 ones for all the kaon experimental sets except for TPC even if the B-factory data are included. Furthermore, the normalization shifts are not as large as the pion factors, and they are 1.03 and 0.96 for Belle and BaBar, respectively, whereas the normalization errors are 1.4% (0.98%) in Belle (BaBar). It indicates that the B-factory kaon data are nearly consistent with previous data, although the normalizations should be still introduced for obtaining sensible results. The first (data) and second (normalization) contributions to χ^2 in Eq. (28) are 18.8=15.0 (1st)+3.8 (2nd) for the Belle and 37.8=21.6 (1st)+16.1 (2nd) for the BaBar. It is noteworthy that the first χ^2 values for the B-factories are very small in the same way with the pion analysis. The data are valuable for determining the kaon FFs. The second normalization contributions to χ^2 are much smaller than the ones for the pion. We show the comparison of the obtained kaon FFs with the data in Fig. 5. We applied the z cut ($z > 0.15$) for the BaBar as explained in Sec. 3.2. In general, the figure shows a good agreement with almost all the data sets within their errors as also indicated by the χ^2 values in Table 2.

In order to illustrate the impact of the B-factory data on the determination of the kaon FFs, the obtained functions are compared with the HKNS07 ones with uncertainties in Fig. 6 (a), and relative uncertainties are shown in (b). There are variations from the previous analysis HKNS07 in the favored functions ($D_u^{K^+}$, $D_{\bar{s}}^{K^+}$). In this analysis, the second moment of the favored one $D_{\bar{s}}^{K^+}$ becomes smaller than the HKNS07 one and it is comparable to the one of the disfavored function $D_d^{K^+}$; however, the moment of $D_{\bar{s}}^{K^+}$ is still larger than the one of $D_d^{K^+}$. We notice in Figs. 4 and 6 that the gluon and heavy-quark (c and b) fragmentation functions

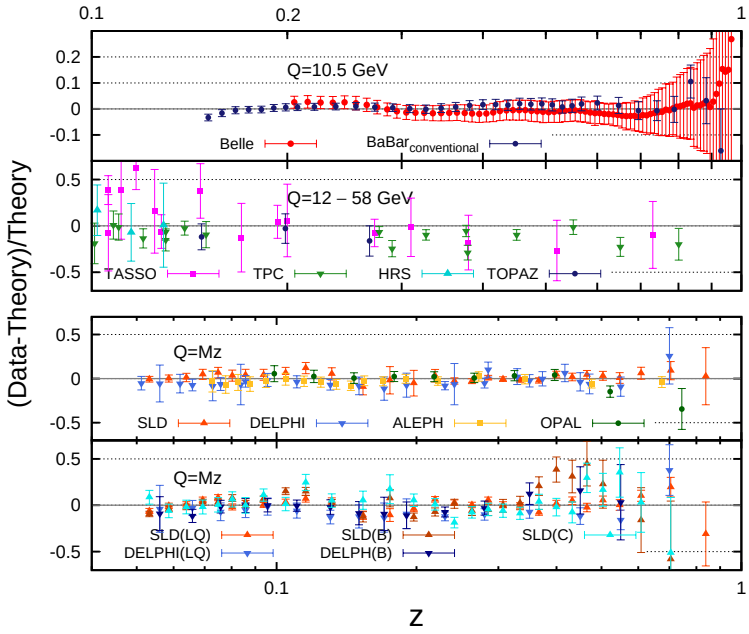

Fig. 5 Comparison of theoretical results at the NLO with charged-kaon production data. The z scale ranges from 0.1 to 1 in the upper two figures (Belle, BaBar; TASSO, TPC, HRS, TOPAZ), and it is from 0.04 to 1 in the lower two figures (SLD, DELPHI, ALEPH, OPAL; SLD(LQ,B,C), DELPHI(LQ,B)).

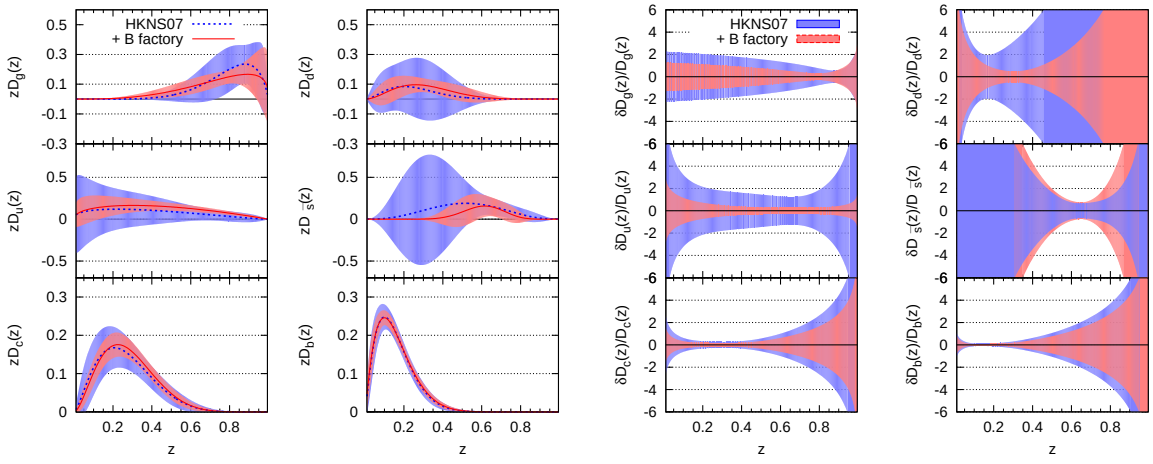

(*a*) (*b*)

Fig. 6 (*a*) Fragmentation functions and their uncertainties are shown for K^+ at Q^2=1 GeV^2, m_c^2, and m_b^2 in the NLO analysis. (*b*) Relative uncertainties are shown. The dashed and solid curves indicate HKNS07 and current (HKKS16) results, and the HKNS07 and HKKS16 uncertainties are shown by the dark- and light-shaded bands, respectively.

of the kaon are shifted toward larger-z regions. It may be interpreted in the following way. In order to create π^+ from g, c, or b, two quark-pair ($u\bar{u}$ and $d\bar{d}$) creations should occur, whereas they are $u\bar{u}$ and $s\bar{s}$ for K^+. Since the s-quark is heavier than d-quark, the initial parton (g, c, or b) should have more energy to fragment into K^+. It means that the function $D^{K^+}_{g,c,b}(z)$ is distributed at relatively larger z than $D^{\pi^+}_{g,c,b}(z)$.

Figures 6 (a) and (b) indicate that the B-factory data significantly improve the determination of the kaon FFs, especially the light-quark and gluon FFs. In the kaon case, we considered two favored functions instead of one favored function in the pion. There are four types: two favored, one disfavored, and gluon functions, in addition to the charm and bottom functions. Considering the current experimental situation, namely accurate data exist mainly at $\sqrt{s} \simeq$10.5 GeV and M_Z, the four independent functions could be considered as redundant for determining all of them simultaneously. It is the reason why the error bands are rather large in comparison with the pion errors. Nonetheless, it is good to obtain more accurate kaon FFs due to the B-factory measurements because the determined FFs are used in kaon-production processes, for example, in probing the strange-quark distribution in the nucleon [42] and strange-quark contribution to the nucleon spin content [43]. Furthermore, accurate measurements of FFs for exotic hadron candidates, such as $f_0(975)$, $a_0(975)$, and $\Lambda(1405)$, could provide valuable information on their internal structure through the favored and disfavored FFs [44].

5. Summary

We analyzed experimental data on hadron productions in electron-positron annihilation, $e^+ + e^- \to h + X$, for determining fragmentation functions. A recent experimental development is that the Belle and BaBar collaborations published high-statistics data on charged pion and kaon productions. In this article, we reported our results on the fragmentation functions of the pion and kaon with uncertainties estimated by the Hessian method in order to show impacts on the B-factory data on the FF determination. The uncertainties are compared between the analysis results and the previous HKNS07 ones without the B-factory information.

It was shown that the B-factory measurements contribute to significant reductions of the uncertainties, especially in the gluon and light-quark fragmentation functions. The B-factory data are taken at $\sqrt{s} \simeq 10.5$ GeV and other accurate data are obtained at 91.2 GeV, so that the scaling violation of the fragmentation functions became clear for the first time. Furthermore, the electric and weak charges are different depending on the quark type, a light-quark flavor separation also became possible. These two factors contributed to a more accurate determination of the gluon and light-quark functions. However, we noticed some tensions between the Belle and BaBar data sets and also between the B-factory and other data sets. The more precise fragmentation functions, by using the Belle and BaBar measurements, could make it possible for finding new physics and the details of nucleon structure at high-energy hadron facilities.

Acknowledgements

The authors thank Martin Leitgab, Matthias Grosse Perdekamp, and Ralf Seidl for communications on Belle measurements, and they thank David Muller for explanations on

BaBar experiments. This work was partially supported by JSPS KAKENHI Grant Numbers, JP21105006, JP25105010, and JP15K05061.

References

[1] M. Hirai, S. Kumano, T.-H. Nagai, and K. Sudoh, Phys. Rev. D **75**, 094009 (2007).

[2] F. Arleo, D. d'Enterria, and A. S. Yoon, JHEP **06**, 035 (2010); B. Abelev *et al.* (ALICE Collaboration), Phys. Lett. B **717**, 162 (2012).

[3] B. A. Kniehl, G. Kramer, and B. Pötter, Nucl. Phys. B **582**, 514 (2000); S. Kretzer, Phys. Rev. D **62**, 054001 (2000); S. Albino, B. A. Kniehl, and G. Kramer, Nucl. Phys. B **725**, 181 (2005).

[4] S. Albino *et al.*, arXiv:0804.2021 [hep-ph]; F. Arleo, Eur. Phys. J. C **61**, 603 (2009); F. Arleo and J. Guillet, online generator of FFs at http://lapth.cnrs.fr/ffgenerator/.

[5] D. de Florian, R. Sassot, and M. Stratmann, Phys. Rev. D **75**, 114010 (2007); **76**, 074033 (2007); T. Kneesch, B. A. Kniehl, G. Kramer, and I. Schienbein, Nucl. Phys. B **799**, 34 (2008); S. Albino, B. A. Kniehl, and G. Kramer, Nucl. Phys. B **803**, 42 (2008); E. Christova and E. Leader, Phys. Rev. D **79**, 014019 (2009); S. Albino and E. Christova, Phys. Rev. D **81**, 094031 (2010). See also B. A. Kniehl and G. Kramer, Phys. Rev. D **74**, 037502 (2006).

[6] M. Epele, R. Llubaroff, R. Sassot and M. Stratmann, Phys. Rev. D **86**, 074028 (2012); D. de Florian, R. Sassot, M. Epele, R. J. Hernandez-Pinto, and M. Stratmann, Phys. Rev. D **91**, 014035 (2015); D. P. Anderle, M. Stratmann, and F. Ringer, Phys. Rev. D **92**, 114017 (2015).

[7] For example, see B. Andersson, G. Gustafson, G. Ingelman, and T. Sjostrand, Phys. Rept. **97**, 31 (1983); Y. Hatta and T. Matsuo, Phys. Lett. B **670**, 150 (2008); T. Ito, W. Bentz, I. C. Cloet, A. W. Thomas, and K. Yazaki, Phys. Rev. D **80**, 074008 (2009); H. H. Matevosyan, A. W. Thomas, and W. Bentz, Phys. Rev. D **83**, 074003 (2011); D **83**, 114010 (2011), Erratum-ibid. D **86**, 059904 (2012); S. Nam and C.-W. Kao, Phys. Rev. D **85**, 034023 & 094023 (2012). D.-J. Yang, F.-J. Jiang, C.-W. Kao, and S. Nam, Phys. Rev. D **87**, 094007 (2013). D.-J. Yang, F.-J. Jiang, W.-C. Chang, C.-W. Kao, and S. Nam, Phys. Lett. B **755** 393 (2016).

[8] X. F. Guo and X. N. Wang, Phys. Rev. Lett. **85**, 3591 (2000); A. Majumder, E. Wang, and X. N. Wang, Phys. Rev. C **73**, 044901 (2006); N. Armesto, L. Cunqueiro, C. A. Salgado, and W. C. Xiang, JHEP **02**, 048 (2008); F. Arleo, Eur. Phys. J. C **61**, 603 (2009); S. Albino, B. A. Kniehl, and R. Perez-Ramos, Nucl. Phys. B **819**, 306 (2009); A. Accardi, F. Arleo, W. K. Brooks, D. d'Enterria, and V. Muccifora, Riv. Nuovo Cimento, **32**, 439 (2010); R. Sassot, M. Stratmann, P. Zurita, Phys. Rev. D **81**, 054001 (2010); W.-T. Deng and X.-N. Wang, Phys. Rev. C **81**, 024902 (2010); R. Dupré, Ph. D. thesis, University of Lyon (2011).

[9] A. Airapetian *et al.* (HERMES collaboration), Nucl. Phys. B **780**, 1 (2007); Phys. Lett. B **684**, 114 (2010); arXiv:1212.5407 [hep-ex].

[10] M. Leitgab *et al.* (BELLE Collaboration), Phys. Rev. Lett. **111**, 062002 (2013); M. Leitgab, Ph. D thesis, University of Illinois at Urbana-Champaign (2013).

[11] J. P. Lees *et al.* (BABAR Collaboration), Phys. Rev. D **88**, 032011 (2013).

[12] R. K. Ellis, W. J. Stirling, and B. R. Webber, *QCD and Collider Physics*, Cambridge University Press (1996).

[13] G. Altarelli, R. K. Ellis, G. Martinelli, and S. Y. Pi, Nucl. Phys. B **160**, 301 (1979); P. Nason and B. R. Webber, Nucl. Phys. B **421**, 473 (1994); Erratum, *ibid.* **480**, 755 (1996). NNLO results are in P. J. Rijken and W. L. van Neerven, Nucl. Phys. B **487**, 233 (1997); A. Mitov and S. Moch, Nucl. Phys. B **751**, 18 (2006).

[14] J. Collins, Nucl. Phys. B **396**, 161 (1993); G. Sterman *et al.*, Rev. Mod. Phys. **67**, 157 (1995).

[15] G. Curci, W. Furmanski, and R. Petronzio, Nucl. Phys. B **175**, 27 (1980); W. Furmanski and R. Petronzio, Phys. Lett. B **97**, 437 (1980); E. G. Floratos, C. Kounnas and R. Lacaze, Nucl. Phys. B **192**, 417 (1981). NNLO results are in A. Mitov, S. Moch, and A. Vogt, Phys. Lett. B **638**, 61 (2006); S. Moch and A. Vogt, Phys. Lett. B **659**, 290 (2008); A. A. Almasy, S. Moch, and A. Vogt, Nucl. Phys. B **854**, 133 (2012).

[16] Relations between the spacelike and timelike splitting functions are discussed in M. Stratmann and W. Vogelsang, Nucl. Phys. **B496** (1997) 41; J. Blumlein, V. Ravindran, and W. L. van Neerven, Nucl. Phys. B **586**, 349 (2000); Y. .L. Dokshitzer, G. Marchesini and G. P. Salam, Phys. Lett. B **634**, 504 (2006). See also articles in Ref. [15].

[17] M. Miyama and S. Kumano, Comput. Phys. Commun. **94**, 185 (1996); M. Hirai, S. Kumano, and M. Miyama, Comput. Phys. Commun. **108**, 38 (1998); **111**, 150 (1998); S. Kumano and T.-H. Nagai, J. Comput. Phys. **201**, 651 (2004).

[18] M. Hirai and S. Kumano, Comput. Phys. Commun. **183**, 1002 (2012).

[19] S. Kumano, Phys. Rept. **303**, 183 (1998); G. T. Garvey and J.-C. Peng, Prog. Part. Nucl. Phys. **47**, 203 (2001); J.-C. Peng and J.-W. Qiu, Prog. Part. Nucl. Phys. **76**, 43 (2014).

[20] R. Brandelik *et al.* (TASSO collaboration), Phys. Lett. B **94**, 444 (1980).
[21] M. Althoff *et al.* (TASSO collaboration), Z. Phys. C **17**, 5 (1983).
[22] W. Braunschweig *et al.* (TASSO collaboration), Z. Phys. C **42**, 189 (1989).
[23] H. Aihara *et al.* (TPC collaboration), Phys. Rev. Lett. **52**, 577 (1984); **61**, 1263 (1988).
[24] M. Derrick *et al.* (HRS collaboration), Phys. Rev. D **35**, 2639 (1987).
[25] R. Itoh *et al.* (TOPAZ collaboration), Phys. Lett. B **345**, 335 (1995).
[26] K. Abe *et al.* (SLD collaboration), Phys. Rev. D **69**, 072003 (2004).
[27] D. Buskulic *et al.* (ALEPH collaboration), Z. Phys. C **66**, 355 (1995); R. Barate *et al.*, Phys. Rep. **294**, 1 (1998).
[28] R. Akers *et al.* (OPAL collaboration), Z. Phys. C **63**, 181 (1994).
[29] P. Abreu *et al.* (DELPHI collaboration), Eur. Phys. J. C **5**, 585 (1998).
[30] P. Abreu *et al.* (DELPHI collaboration), Nucl. Phys. B **444**, 3 (1995).
[31] http://hepdata.cedar.ac.uk/review/ee/.
[32] S. Albino, B.A. Kniehl, G. Kramer, and W. Ochs, Phys. Rev. D **73**, 054020 (2006).
[33] W. Furmanski and R. Petronzio, Z. Phys. C **11**, 293 (1982).
[34] F. Halzen and A. D. Martin, *Quarks and Leptons: An Introductory Course in Modern Particle Physics*, John Wiley & Sons (1984).
[35] J. Beringer *et al.* [Particle Data Group Collaboration], Phys. Rev. D **86**, 010001 (2012).
[36] A. D. Martin, R. G. Roberts, W. J. Stirling, and R. S. Thorne, Eur. Phys. J. C **23**, 73 (2002); Phys. Lett. B **531**, 216 (2002).
[37] For example, see G. D'Agostini, Nucl. Instrum. Meth. A **346**, 306 (1994); R. D. Ball *et al.* (NNPDF Collaboration), JHEP **05**, 075 (2010).
[38] F. James, CERN Program Library Long Writeup D506 in https://root.cern.ch/sites/d35c7d8c.web.cern.ch /files/minuit.pdf; see also https:www.cern.ch/minuit.
[39] J. Pumplin *et al.*, Phys. Rev. D **65** (2001), 014012 & 014013; A. D. Martin *et al.*, Eur. Phys. J. C **28** (2003), 455; **35** (2004), 325.
[40] M. Hirai, S. Kumano, and N. Saito, Phys. Rev. D **69** (2004), 054021; D **74** (2006), 014015; M. Hirai and S. Kumano, Nucl. Phys. B **813** (2009), 106; M. Hirai, S. Kumano, and T.-H. Nagai, Phys. Rev. C **70** (2004), 044905; **76** (2007), 065207.
[41] For example, see https://cern-tex.web.cern.ch/cern-tex/minuit/node33.html, http://pdg.lbl.gov/2015 /reviews/rpp2015-rev-statistics.pdf.
[42] A. Airapetian *et al.* (HERMES Collaboration), Phys. Lett. B **666**, 446 (2008); Phys. Rev. D **89**, 097101 (2014); W.-C. Chang and J.-C. Peng, Phys. Rev. Lett. **106**, 252002 (2011); H. Kawamura, S. Kumano, and Y. Kurihara, Phys. Rev. D **84**, 114003 (2011).
[43] E. Leader, A. V. Sidorov, and D. B. Stamenov, Phys. Rev. D **84**, 014002 (2011).
[44] M. Hirai, S. Kumano, M. Oka, and K. Sudoh, Phys. Rev. D **77** (2008), 017504.